UDC 534.121.1

V.L. Karlash, Dr.Sc.
S. P. Timoshenko Institute of Mechanics, Nat. Acad. Sci. of Ukraine,
3, Nesterov Str. 03057, Kyiv, Ukraine, e-mail: karlashv@ukr.net.

Energy losses in piezoceramic resonators and its influence on vibrations' characteristics

This paper is devoted to analyze of the modern achievements in energy loss problem for piezoceramic resonators. In parallel a new simple methodic of an experimental determination of energy losses and coupling coefficients is presented and author's opinion why mechanical quality is different on resonance and anti-resonance is gave. The reason lies in "clamped" capacity and electromechanical coupling factor's value. The better electromechanical coupling the stronger capacity "clamping" and the higher its influence on anti-resonant frequency and quality. Reference 36, figures 4, tables 3.

Keywords: *piezoceramic resonators, energy losses, electromechanical coupling factors, resonance/anti-resonance mechanical quality.*

Introduction

Piezoceramic construction elements, while performing similar or better than electromagnetic ones, are more suitable for miniaturization's purpose [31 – 33]. When uniform mechanic stress is applied in a non-center symmetric crystal or polarized piezoceramic's sample there is a movement of positive and negative ions with respect to each other, creating an electric charge at the surface. This is a direct piezoelectric effect – a conversion of mechanical energy into electrical energy. When electric field is applied to the sample an elastic strain is produced. This is a converse piezoelectric effect – a conversion of an electric energy into mechanical energy. When an alternating electric field is applied mechanic vibrations are induced, which at appropriate frequency cause mechanical resonance with great strains and stresses. A phenomenon of strain increasing due to accumulated electric energy is called a piezoelectric resonance [1, 6, 9, 13, 28, 29]. Both direct and converse piezoelectric effects are linear physical phenomena with respect to induce fields.

The internal physical processes nature in piezoceramic constructive elements drives to the fact that displacements, strains, stresses, admittance and impedance have both real and imaginary parts [9, 13, 14, 28, 29]. It is impossible to calculate any amplitude without accounting the energy losses [13, 29]. The electromechanical coupling firstly was introduced in analyze by W. Voigt [35]. An energy losses problem appears in pioneer's works of a XX-th century beginning of S. Butterworth [2]; W. G. Cady [3]; K. S. Van Dyke [5]; S. L. Quimby [27]; D. E. Dye [4] etc. Energy losses were accounted as viscosity, decaying decrements or acoustic radiation. Later W. P. Mason introduced in equivalent electric network an additive loss resistor [22]. In 60-th and 70-th years an idea of complex coefficients was proposed and back-grounded by S. E. Land *et al* [21], G. E. Martin [23], R. Holland [7] etc. In analyze energy losses now include three imaginary parts: elastic, dielectric and piezoelectric ones [7, 9, 13, 23, 28, 29] Loss problem especially rises in high frequency (20 – 100 MHz) applications where thickness reaches 200 mkm or less [24].

The analytic solutions for electroelastic vibrations of simple geometric form bodies such as bars, rods, disks, circular or cylindrical rings etc [7, 13, 23, 28] are used in standards for determining real parts of the dielectric, elastic and piezoelectric coefficients [6, 8, 28]. Imaginary parts usually are determined on maxima / minima admittance, first proposed by Martin [23]. In [11, 12].it was proposed to use for such aims thin piezoceramic disk's radial vibrations. Very important role in energy losses belongs to mechanic quality factor *Q*, which differs for resonance and anti-resonance [25, 26].

An investigation of energy losses in piezoelectric materials was, is and will be during long time with important scientific problem

Elastic, dielectric and piezoelectric energy losses in piezoceramics and their measuring

In analyze the piezoceremic elements are described by various elastic, dielectric and piezoelectric coefficients or modulus, which are represented mostly in complex form [7, 9, 14, 29]

$$a = a_1 - ja_2 = a' - ja'' = a_{10}(1 - ja_{1m}); \qquad \frac{a_2}{a_1} = \frac{a''}{a'} = a_{1m} = \tan\xi. \tag{1}$$

Here in common view as *a* it is noted such electroelastic coefficients as stiffness c_{ij}, compliances s_{kl}, piezomodulus d_{nm}, coupling factors k_{tr},

dielectric constants ε_{pq} etc. Expressions for elastic displacements *U*, strains ε and stresses σ, electric powers *P*, admittances *Y* or impedances *Z*, dimensionless frequencies *x* are complex too [13]. For imaginary parts of complex modulus were derived next restricting inequalities [7, 9, 28]

$$\begin{gathered} s''_{11}, s''_{33}, s''_{44}, s''_{66}, \varepsilon''_{11}, \varepsilon''_{33} \ge 0; \\ s''_{11} \ge |s''_{12}|; \\ s''_{11} s''_{33} \ge (s''_{13})^2; \\ s''_{11} \varepsilon''_{33} \ge (d''_{31})^2; \\ s''_{33} \varepsilon''_{33} \ge (d''_{33})^2; \\ s''_{33}(s''_{11} + s''_{12}) \ge 2(s''_{13})^2; \\ \varepsilon''_{33}(s''_{11} + s''_{12}) \ge 2(d''_{31})^2. \end{gathered} \quad (2)$$

All notations are taken from [13, 29]. These inequalities show that energy losses imaginary parts in *piezoelectric* materials are not random but are coupled each other. It means that perfect in elastic or dielectric properties piezoelement has perfect electroelastic properties too.

Analytic calculations and experimental data show that losses influences on vibrations are different at resonance/anti-resonance phenomena. All modern methods of loss tangents determination base on maxima/minima admittance measure at first rod or bar mode of vibration [7, 24].

It may be shown that piezoelectric resonator's admittance is inter-electrode capacity C_0 conductivity produced on anti-resonance $\Delta_a(x)$ to resonance $\Delta(x)$ determinants ratio

$$Y = j\omega C_0 \frac{\Delta_a(x)}{\Delta(x)}, \quad (3)$$

x – is dimensionless frequency, which depend upon geometric sample's form.

Next formulae were derived for thin rod with thickness polarization, shot cylindrical ring and high cylindrical shell with radial polarization accordingly [28]

$$Y_b = j\omega C_0 \left[1 - k_{31}^2 + \frac{k_{31}^2 \sin x}{x \cos x} \right] = j\omega C_0 \frac{\Delta_a(x)}{\Delta(x)}, \quad (4)$$

$$\Delta(x) = \cos(x), \Delta_a(x) = (1 - k_{31}^2)\Delta(x) + k_{31}^2 \sin x / x$$

$$Y_{sk} = j\omega C_0 \left[1 - k_{31}^2 + \frac{k_{31}^2 \omega_r^2}{\omega_r^2 - \omega^2} \right] = j\omega C_0 \frac{\Delta_a(x)}{\Delta(x)}, \quad (5)$$

$$\Delta(x) = \omega_r^2 - \omega^2, \Delta_a(x) = (1 - k_{31}^2)\Delta(x) + k_{31}^2 \omega_r^2$$

$$Y_{hk} = j\omega C_0 \left[1 - k_p^2 + \frac{(1+\nu) k_p^2 \omega_r^2}{2(\omega_r^2 - \omega^2)} \right] = j\omega C_0 \frac{\Delta_a(x)}{\Delta(x)}, \quad (6)$$

$$\Delta(x) = \omega_r^2 - \omega^2, \Delta_a(x) = (1 - k_p^2)\Delta(x) + (1+\nu) k_p^2 \omega_r^2 / 2.$$

Here: *j* is an imaginary unit, ω is an angular frequency, ω_r – resonant angular frequency, k_{31} – transverse coupling coefficient, k_p – planar coupling coefficient, ν - Poisson ratio.

After substituting (1) in (4) G. E. Martin obtained approximate formulae [23]

$$\begin{gathered} Y_m = \frac{8\omega_m C_0 k_{31}^2}{\pi^2 s_{11m}}, \\ Y_n = \omega_n C_0 \left[\varepsilon_{33m} - 2d_{31m} + \frac{\pi^2 s_{11m}}{8k_{31}^2} \right] \end{gathered} \quad (7)$$

and

$$\begin{gathered} s_{11m} = \frac{16 f_m C_0 k_{310}^2}{\pi Y_m}, \\ d_{31m} = \frac{\varepsilon_{33m}}{2} + \frac{\pi^2 s_{11m}}{16 k_{310}^2} - \frac{Y_n}{4\pi f_n C_o} \end{gathered}. \quad (8)$$

Coupling coefficient k_{31} is determined as [26, 28]

$$\frac{k_{310}^2}{1 - k_{310}^2} = \frac{\pi}{2} \frac{f_n}{f_m} \tan\left[\frac{(f_n - f_m)\pi}{2 f_m} \right]. \quad (9)$$

In a "short" cylindrical ring case dimensionless frequency is $x = \omega / \omega_r$ and coefficient k_{31} is determined from relation

$$k_{310}^2 = \frac{\omega_a^2 - \omega_r^2}{\omega_a^2}, \quad (10)$$

known as Meson's formula [1, 6, 15, 28]. Maxima admittance and mechanic quality are

$$\begin{gathered} Y_m = \omega_m C_0 k_{310}^2 Q_m = \frac{\omega_m C_0 k_{310}^2}{s_{11m}}, \\ Q_m = \frac{Y_m}{\omega_m C_0 k_{310}^2}. \end{gathered} \quad (11)$$

In a "high" cylindrical ring case dimensionless frequency is $x = \omega/\omega_r$ and coefficient k_p is determined from relation

$$\frac{2(1 - k_p^2)}{(1+\nu) k_p^2} = \frac{f_m^2}{f_n^2 - f_m^2}. \quad (12)$$

Thin piezoceramic disk's radial vibrations have following admittance [9, 13, 29]

$$\begin{gathered} Y_{dsk} = j\omega C_0 \left[1 - k_p^2 + \frac{(1+\nu) k_p^2 J_1(x)}{\Delta(x)} \right] = j\omega C_0 \frac{\Delta_a(x)}{\Delta(x)}, \\ \Delta(x) = x J_0(x) - (1-\nu) J_1(x), \\ \Delta_a(x) = (1 - k_p^2)\Delta(x) + (1+\nu) k_p^2 J_1(x). \end{gathered} \quad (13)$$

Dimensionless frequency for disk is $x = \omega R \sqrt{\rho s_{11}^E (1 - \nu^2)}$, where *R* – is plate's radius, ρ - density.

After manipulating with complex functions, in [12, 13, and 29] it was obtained

$$s_{11m} \approx \frac{4.9 f_{m1} C_0 k_{po}^2}{Y_{m1}}, d_{31m} \approx \frac{s_{11m} + \varepsilon_{33m}}{2} - \\ - \frac{Y_n}{4\pi f_{n1} C_0} + \frac{s_{11m} x_n \delta_n}{4\Delta_n} \\ \delta_n = (1 + k_{p0}^2)\beta_n + k_{p0}^2 (1 + \nu)\gamma_n; \\ \gamma_n = [x_n J_0(x_n) - J_1(x_n)] / x_n; \\ \beta_n = (1 + \nu) J_0(x_n) - \kappa_0 J_1(x_n) - \\ - \Delta(x_n) / x_n, \Delta_n = \Delta_a(x_n) \quad (14)$$

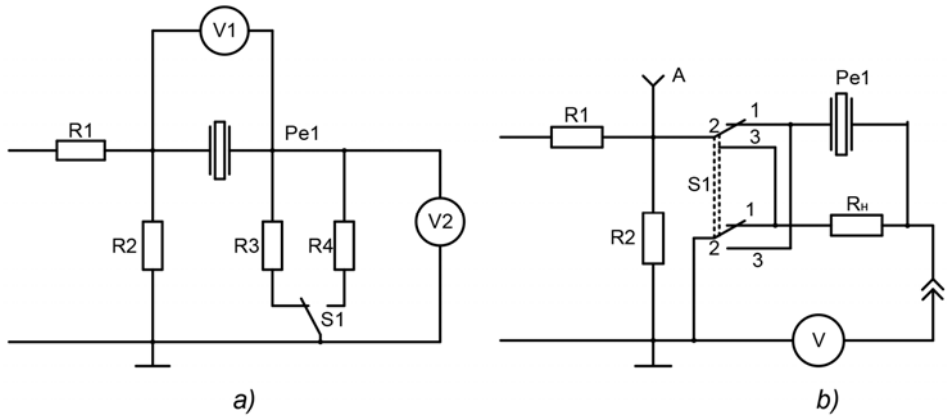

Fig. 1. Meson's four-pole variants

To use these formulae it is necessary to measure maxima/minima admittances and frequencies and to calculate factors β, δ, γ at anti-resonance.

The resonance and anti-resonance frequencies are determined in analyze as that frequencies, where phase shifts between sample's voltage and its current are zero [1 – 3, 6]. It is not lightly to reach such effect in practice, and resonant frequency f_r is identified with maxima admittance frequency f_m, while anti-resonant frequency f_a is identified with minima admittance frequency f_n.

Two variants of simple experimental networks are presented on Fig 1. The first schema is known as Meson's four-pole [6, 9, 13]. Input voltage divider *R1,R2* matches generator's output with measuring circuit. In parallel to output resistor *R2* is included piezoelement *Pe* and loading resistors *R3* or *R4*. Voltmeter *V1* measures voltage U_{pe} dropped on piezoelement and voltmeter *V2* measures voltage U_R dropped on loading resistors Voltage U_R is proportional to electrical current I_{pe} in resistor and sample. The ratio of current to voltage is definite as admittance, so that

$$Y_{pe} = \frac{I_{pe}}{U_{pe}} = \frac{U_R}{R U_{pe}}. \quad (15)$$

In practice formula (15) not may be used in Fig 1, *a* schema, because do not exist such voltmeter, which may be taken for *V1* position. On this reason voltage U_{pe} in this schema determined as difference between input voltage U_{in} and voltage U_R. Instead of the exact formula (15) an approximation is used

$$Y_{pe1} = \frac{U_R}{R(U_{in} - U_R)}. \quad (16)$$

When loading resistor and sample change one another, a next approximate formula may be derived

$$Y_{pe2} = \frac{(U_{in} - U_{pe})}{R U_{pe}}. \quad (17)$$

In contrast, the Fig 1, *b* network permits to measure all voltages $U_{pe,}$ U_{in} and U_R in a wide frequency range by single voltmeter *V* [15]. Voltmeter's input (point "*C*") may be connected with voltage divider's output (point "*A*") or common for resistor and sample connection (point "*B*"). In higher switcher's position, as shown on Fig 1, *b*, this network is analog to Fig 1, *a* schema and voltmeter measures U_R voltage. When switcher *S1* is in lower position, voltmeter measures U_{pe} voltage. This

schema is able to realize three various loading conditions: 1) constant current, 2) constant sample's voltage, 3) constant input voltage. Experimental data enter to PC and AFCh (amplitude-frequency characteristics) a number of physical parameters are plotted.

Table 1. Dependence of an admittance maxima and resonant frequency upon loading resistor's value

R_l, Ohm	1,6	5,3	11,2	230	993
f_r, kHz	31,572	31,560	31,562	31,563	31,576
Y_m, mS	131,4	124	119,6	101,4	26,36

Table 1 shows that frequencies of admittance maxima have very small dependencies upon loading resistor value but strong for conductivity.

Three measured voltages U_{pe}, U_R and U_{in} create peculiar characteristic triangle and angles between its sides may be calculated with using a cosine theorem (*low of cosines*) as

$$\cos\alpha = \frac{U_{pe}^2 + U_R^2 - U_{in}^2}{2U_{pe}U_R},$$
$$\cos\beta = \frac{U_{in}^2 + U_R^2 - U_{pe}^2}{2U_{in}U_R}, \quad (18)$$
$$\cos\gamma = \frac{U_{in}^2 + U_{pe}^2 - U_R^2}{2U_{in}U_{pe}}$$

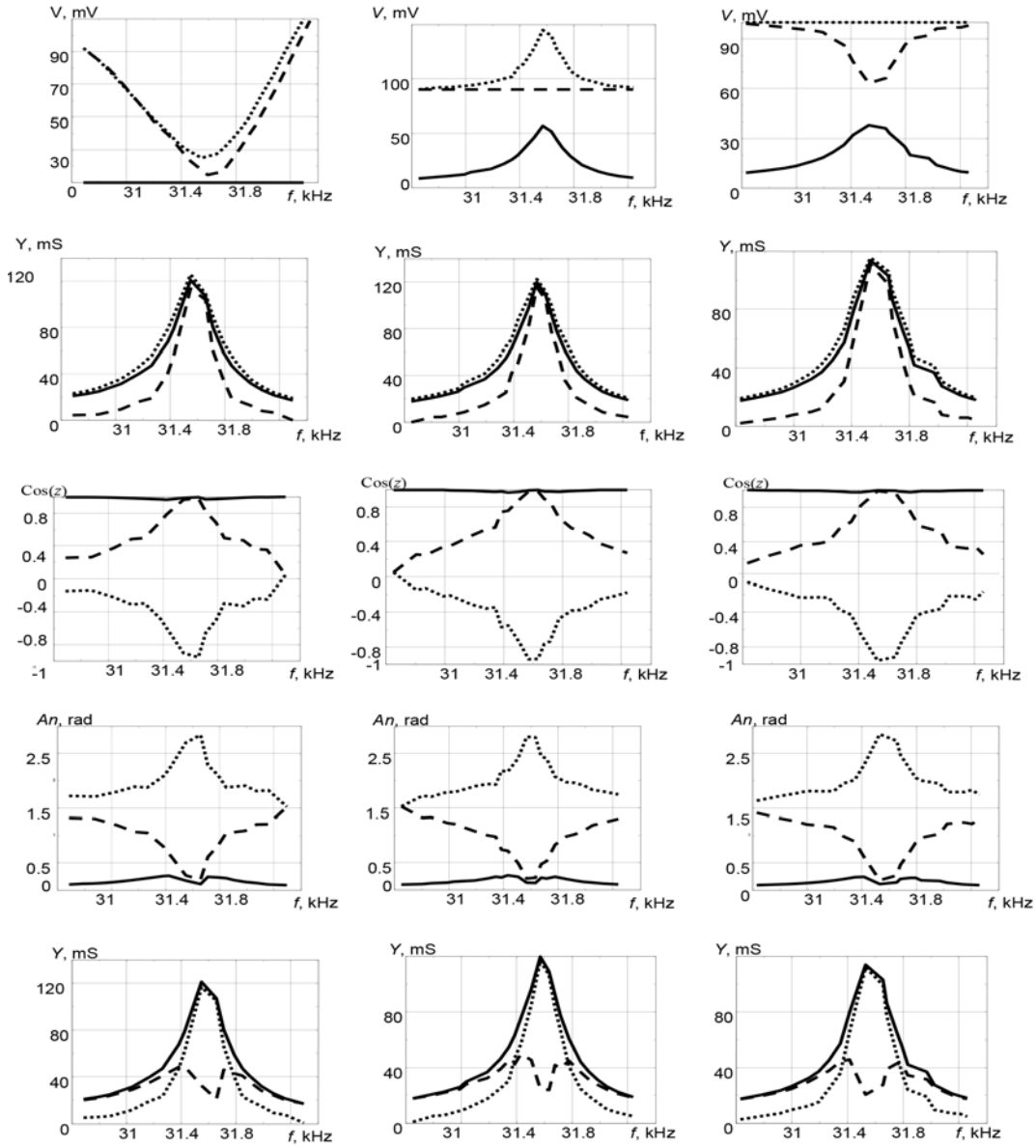

Fig. 2. AFCh of voltages, admittances and angles in piezoelectric disk

Fig.2 demonstrates AFCh of voltages U_{pe}, U_R and U_{in} (in milliVolts), full admittance (in milliSimens), cosines, angles (in radians) and admittance's components. Graphs are obtained for constant current amplitude I_{pe} =U_R /R=1,89 mA (left), constant voltage amplitude U_{pe} =90 mV (centre) and constant input voltage amplitude U_{in}=100 mV (right) conditions near first radial resonance of TsTBS-3 disk 66,4 x 3,1 mm with such parameters: C_0=18,5 nF, dielectric loss tangent ε_{33m} =0,0085; mechanical loss tangent s_{11m} =0,0069); Poisson ratio ν=0,35; planar EMCF square k_{po}^2 =0,31 and piezoelectric loss tangent d_{31m} =0,0076.

On higher graphs (first row) U_{pe} are shown as interrupted curves, U_{in} – as dot curves and U_R as unbroken lines. Full admittances (second row) are calculated with formulae (15) (unbroken lines), (16) (dot lines) and (17) (interrupted curves). At resonance exact (15) and approximate (16, 17) expressions gave the same results. Third and forth rows present cosines of triangle's angles and corresponding angles. Angle α (dot lines) is created by U_R and $U_{pe,}$ sides. It characterizes a phase shift between piezoelement's current and voltage. Angle β (interrupted curves) is created by sides U_{in} and $U_{R.}$ It is according to phase shift between output generator voltage and consuming current. At least, angle γ (unbroken lines) is created by sides U_{in} and U_{pe}, i. e. between output generator voltage and sample's voltage. Lower, fifth row presents full Y (unbroken curves), real G (dot lines) and imaginary B (interrupted curves) parts of admittance, calculated with formulae, which give same results
or

$$G_2 = Y_{pe} / \sqrt{(1+k^2)}, \qquad B_2 = G_2 k, \; k = \tan\beta \tag{20}$$

Graphs of Fig.2 show that for small signal appropriate circumstances constant current and constant voltage exhibit same result.

Experimental methodic of loss characteristics determination in our time is such as 50 years ago. At a low frequency (1000 Hz or near) capacity bridge measures inter-electrode capacity C_0 and tan δ=ε_{33m}. Maxima / minima admittances are used then for calculations of elastic s_{11m} and ptezoelectric d_{31m} loss tangent with formulae (8) forrods or (14) for disks. Mechanical tangent s_{11m}=1/Q_m is determined too by bandwidth method from AFCh admittance [25] or transform ratio in piezotransformer transducer method [16]. A piezotransformer transducer method bases on dividing in electrode piezoelement surface one or a number of small parts and in measuring their potentials or charges, which are proportional to inner mechanical stresses.

Plotting a dependence of potentials such transducers in any surface direction we may study a stress state on resonance frequencies. Plotting AFCh of such transducer's potentials U or transform ratio K_t=U/U_0 (U_0 is input voltage) we may determine mechanical quality factor

$$Q_m = \frac{f_9}{f_2 - f_1}, \tag{21}$$

where: f_0 – maximum potential frequency, $f_2 - f_1$ – difference between –3db level frequencies, which lie upper and lower f_0.

It is sufficient difference between constant current and constant voltage loading conditions for high power regime devices, such as radiators, ultrasonic motors or transformers. Recently C.O. Ural *et al* [33] show that constant voltage regime is surrounded with great nonlinearity while constant current regime don't exhibits its. Data were obtained from longitudinal first mode rectangular PZT–8 plate vibration. Authors consider that there is serious difficulty in determining the electromechanical coupling parameters under a high electric field drive from the admittance curves under a constant voltage condition. With a constant voltage method the resonance spectrum distorts significantly, sometimes exhibiting large hysteresis or a jump of the peak curve upon rising and falling frequency driving. Careful analyze of [33] graphs shows that maxima admittance for constant voltage conditions reach 50 mS only while at constant current it reach 80 mS. The maxima admittance frequencies lie in first case in range 55,9 – 56,1 kHz and in range 56,2 – 56,4 kHz for second case. It means that power and temperature conditions at constant voltage and constant current regime are not identical.
Simple calculations on [33] graphs data (Table. 2, Table 3) show that constant voltage condition differs from constant current condition with maxima power level a number of times.

Table 2. Power's maxima at constant voltage conditions

U, mV	100	300	500	800	1000	1500
I, mA	4,9	14,7	29,5	33,6	37	40,5
P, mW	0,49	4,41	11,75	26,8	37	60,7

Table 3. Power's maxima at constant current conditions

I, mA	5	10	20	30	40
U, mV	71,5	131	266	400	558
P, mW	0,36	1,31	5,33	12	23,5

To examine the energy loss tangent's influence on vibration characteristics the calculations were provided near maxima admittance / impedance for TsTBS-3 disk 66,4 x 3,1 mm. Formulae (13) were used in complex form (without Bessel function expansions) for dimensionless frequency ranges 2,05–2,1; 2,39–2,415, k_p^2=0,32, s_{11m}=0,007, ε_{33m}=0,0085, and for three values d_{31m}=0,0035; 0,005 and 0,007. All three admittance curves coincide – dielectric and piezoelectric losses don't influence on resonant vibrations near first resonance. It was obtained such values Y_{m0}=132 mS, $Y_{1,2}$=93,3 (on bandwidth ends –3 dB level [25, 31]), x_0=2,079, Q_r=138–148. Impedance lines differ in amplitude and have such bandwidth method determined qualities Q_a=228,4; 184,5 and 171,4. In experiment loading resistor near resonance was 11,2 Ohm and near anti-resonance – 20 kOhm. It was obtained such results: Y_m=127,1 mS, Y_{-3db}=89,87≅90 mS; f_2–f_1=22/28*300=235,7 Hz; Q_r=31551/235,7=138,8; Z_n=16,86 kOhm, Z_{-3db}=11,92 kOhm; f_2–f_1=31/33*200=187,9 Hz; Q_a=36,499/187,9=194,2. The results are in a good matching with calculated data and show that resonant and anti-resonant quality factors differ almost 40 % while in calculations were taken constant value for mechanical quality equal Q_m=143. It means that conception of constant (frequency independent) values of dielectric, elastic and piezoelectric loss tangent do not conflict with analytic and experimental results.

Independence resonant phenomena upon dielectric and piezoelectric losses was postulated by G.W.Katz [20] for Rozen-type [34] transformer and was used in my papers [17 – 19]

A new methodic for determination coupling and loss coefficients

The procedure of coupling and loss coefficients determination may be simplified and its accuracy may be increased by calculation of full admittance's AFCh in frequency range near resonance and anti-resonance. The methodic is described below on example of thin piesoceramic disk's radial vibrations but it may be provided with similar success for somewhat geometry form elements with famous resonant/anti-resonant determinants. At first the resonance/anti-resonance frequencies and admittances are measured for first and second vibration modes as well as static capacity C_0 and dielectric loss tangent ε_{33m}. Ratio f_{r2}/f_{r1} gives Poisson ratio ν [6, 9, 13, 28] and a ratio f_{a1}/f_{r1} gives planar EMCF k_p^2 [6, 13, 29]. Mechanical quality Q_m is found by piezotransformer transducer method [13, 29] or in another way and elastic loss tangent s_{11m} is found as

$$s_{11m} = \frac{1}{Q_m}. \qquad (22)$$

Values s_{11m}, ε_{33m}, ν, C_0 and k_p^2 as well as $d_{31m}\approx\varepsilon_{33m}$ (this parameter is not known at first and its value is taken randomly) enter to PC. Admittance AFCh in first resonance vicinity is plotted. A ratio maxima/minima frequency is compared with measured one and k_p^2 is correlated. Admittance AFCh in first resonance vicinity is plotted again and s_{11m} is correlated. When calculated values of Y_m and f_{a1}/f_{r1} coincide with measured ones it may be go to anti-resonant region and to find a piezoelectric loss tangent. Author's experience shows that good results are obtaining with three or four iterative steps. For first step any hypothetic data may be taken of cause.

Let us look an example (Fig. 3). To admittance calculation convenience it is doubt to present ωC_0 as

$$\omega C_0 = \frac{2\pi f_0 C_0 x}{x_0} = ax, \quad a = \frac{2\pi f_0 C_0}{x_0}, \qquad (23)$$

here: f_0 is resonance frequency, x_0 – dimensionless resonant frequency (first resonant determinant root), x – running dimensionless frequency.

The first step (Fig 3, *a*) was made with next data (disk TsTBS-3 66,4x3,1 mm size) a=1.77, ν=0,35, ε_{33m}=0,0085, k_p^2=0,2, s_{11m}=0,01; d_{31m}=0,01 Measured frequency ratio was 36502/31560=1,156, calculated – 2,27/2,08=1,091. It is necessary to increase k_p^2 value. For the case k_p^2=0,3 (Fig 3, *b)* frequency ratio is 2,38/2,08=1,144, and for case of k_p^2=0,32 (Fig 3, *c*) f_{a1}/f_{r1}=2,4/2,08=1,154. This result is almost equal to measured one. The calculated 92 mS and measured 131 mS maxima admittance differ in 1,42 times and elastic loss tangent must be decreased to s11m=0,007 (Fig 3, *d*). Now calculated and experimental admittances at resonant frequency are agreed and may be work next step and go to admittance minima (Fig 3, *e*).

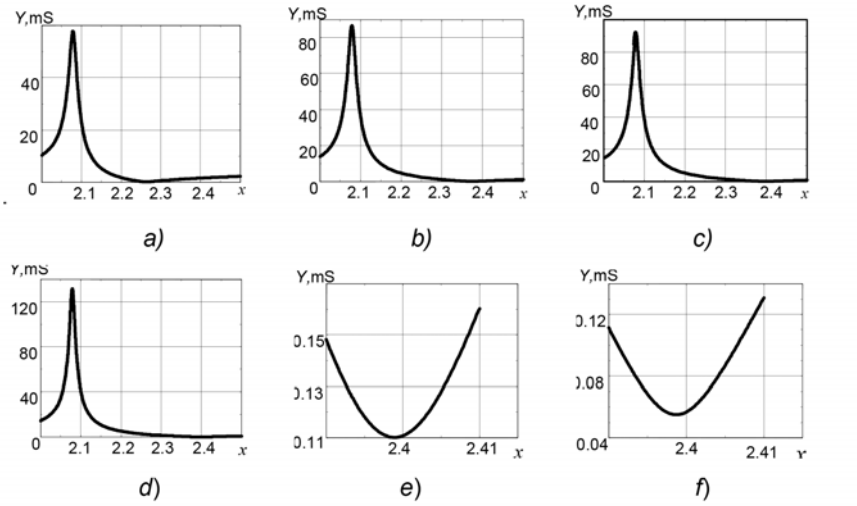

Fig. 3. Steps of iterative methodic

Graph's minimum is 0,11 mS but in experiment it is 0,0587 mS for loading resistor value 20 kOhm. Decreasing of piezoelectric loss tangent to a level d_{31m}=0,0035 decreases admittance minimum to value Y_n=0,056 мS (Fig 3, *f*), that is in a good matching with an experiment

As a result of describing investigations for called higher disk 66,4x3,1 mm from TsTBS-3 material the next refined data were obtained:

$$k_{31}^2=\frac{(1-\upsilon)}{2}k_p^2,\quad \frac{1}{s_{11}}=\frac{\pi^2 d^2 f_m^2(1-\upsilon^2)\rho}{\kappa_1^2},\quad d_{31}=k_{31}\sqrt{\varepsilon_{33}s_{11}},g_{31}=\frac{d_{31}}{\varepsilon_{33}}. \qquad (24)$$

Here: *d* is plate diameter, κ_1 – root of resonance determinant (14).

Dielectric constant is determined from a plate capacitor formula

$$\varepsilon_{33}=4hC_0/\pi d^2 \qquad (25)$$

and for our disk it is $\varepsilon_{33}=\frac{4*2*10^{-3}*51{,}1*10^{-9}}{\pi*100*100*10^{-6}}$ Ф/м=$130{,}2*10^{-10}$; Ф/м=$1471\varepsilon_0$.

Results and discussion

Vibrating system for any piezoelectric resonator may be presented an equivalent electrical network in which in parallel to static inter-electrode capacity C_0 is connected a series branch, consisting from inductance *L,* capacitor *C* and resistor *r* (this resistor symbolizes elastic energy losses). Such system is called in radio-engineering as third view circuit [10]. A voltage resonance in series circuit corresponds to resonant frequency when $r=1/Y_m$. And the current resonance in parallel circuit corresponds to anti-resonant frequency. This parallel circuit consists from inductance *L* and equivalent condenser *C'*, which created by C_0 and C in series $C'=C_0\,C/(C_0+C)$.

In radio-engineering quality *Q* of resonant system determined as ratio of stored in circuit energy E_{stor} to loss energy $E_{dis.av}$ which dissipate during vibration period. It expressed with circuit parameters in such a way [10, 36]

$$Q=2\pi\frac{E_{stor}}{E_{dis.av}}=\frac{\rho}{r}=\frac{2\pi f_0 L}{r}=\frac{1}{2\pi fC},\rho=\sqrt{\frac{L}{C}},f_0=\frac{1}{2\pi\sqrt{LC}}, \qquad (26)$$

is wave circuit resistance, *r* – loss resistor, f_0 – resonant frequency, *L* and *C* – circuit inductance and capacity.

The next formulae may be obtained

$$C=\frac{1}{\rho\omega}=\frac{1}{2\pi f_0\rho}=\frac{1}{2\pi f_0 Q_r r},L=\frac{\rho}{\omega}=\frac{\rho}{2\pi f_0}=\frac{Q_r r}{2\pi f_0}. \qquad (27)$$

In our disk 66,4*3,1 мм, loading on 11,2 Ohm, loss resistor was r=7,87 Ohm, Qr=138,8 and ρ=Qr*r=1092 Ohm, f0=3,155*104, C0=1,849*10-8 F. Substituting these data in (27) we may obtain C =1/(2*3,14*1,092*3,155*107)F=1/(2,164*108)F= =4,62*10-9 F, L=1092/(2*3,14*3,155*104)= =5,51*10-3 Hn. Parallel circuit capacity is C'=C*C0 /(C+C0)=4,62*18,49/(4,62+18,49)*10-9

F=3,696*10-9 F. Parallel resonance frequency, wave resistance and anti-resonant quality factor are f_n=3,528*10^4 Hz, ρ= =1221 Ohm, Q_a=1221/7,87=155,1. Measured values were next 36 499 Hz, Q_a =194,2.

Why so great discrepancy between calculated and measured values of qualities and anti-resonant frequencies exists? The reason lies in clamped capacity and electromechanical coupling factor's values. The better electromechanical coupling the stronger capacity clamping and the higher its influence on anti-resonant frequency and quality. In our disk case k_p^2=0,32 and C_{0c}=(1-k_p^2) C_0 =0,68*1,849* *10^{-8} F=1,257*10^{-8} F. After such correction we have C_1'=4,62*12,57/(4,62+12,57)*10 ^{9} F=3,378*10 $^{-9}$ F, f_n=3,69*10^4 Hz, ρ=1277 Ohm, Q_a=1277/7,87= =162,3. Frequency difference now is 0,9 %, quality difference – 16,4 %

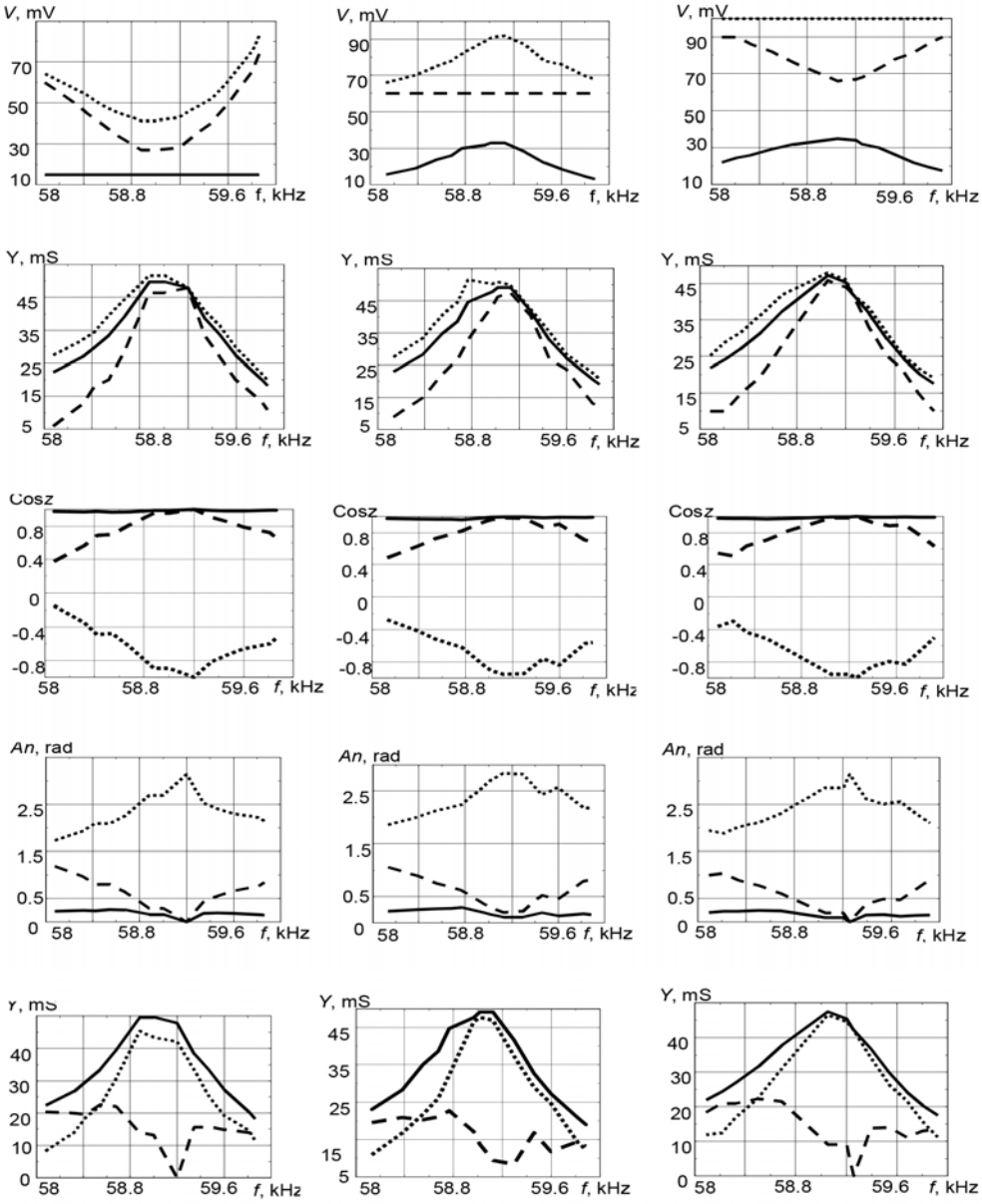

Fig. 4. AFCh of voltages, admittances and angles in equivalent network

Fig 4 rerpresents a result of modeling equivalent network with L=0,4 mHn, C_0=9,579 nF, C= =1,814 nF and R=11,2 Ohm Graphs are plotted for voltages, input admittance, cosines, angles and real/imaginary admittance. Graphs are obtained for constant current I_{eq} =U_R /R=15 mV /11,2 Ohm= =1,34 mA (left), constant voltage U_{eq}=60 mV (centre) and constant input voltage U_{in}=100 mV (right) conditions near series circuit resonance.

On higher graphs (first row) U_{eq} are shown as interrupted curves, U_{in} – as dot curves and U_R as unbroken lines. Full admittances (second row) are calculated with formulae (15) (unbroken lines), (16) (dot lines) and (17) (interrupted curves). Third and

forth rows present cosines of triangle's angles and corresponding angles. Angle α (dot lines) is created by U_R and $U_{eq,}$ sides. It characterizes a phase shift between circuit's current and voltage. Angle β (interrupted curves) is created by sides U_{in} and $U_{R.}$ It is according to phase shift between output generator voltage and consuming current. At least, angle γ (unbroken lines) is created by sides U_{in} and U_{eq}, i. e. between output generator voltage and equivalent circuit's voltage. Lower, fifth row presents full *Y* (unbroken curves), real *G* (dot lines) and imaginary *B* (interrupted curves) parts of circuit admittance, calculated with formulae (19) or (20). Graphs of Fig.4 in general are similar to lines of Fig 2. Both show that for small signal appropriate circumstances constant current and constant voltage exhibit same result.

Conclusions

Analysis of the efficiency of excitation at resonance/anti-resonance frequencies was made by many authors. It was established [25, 26] that the character of the interrelation of quality factors is determined mainly by the imaginary part of electromechanical coupling factor whose influence is the most essential at the fundamental anti-resonance frequency. Greater value of the anti-resonance quality factor in respect to the resonance quality factor makes it preferable to provide the top mechanical displacement amplitude. The piezoelectric loss tangent causes changes not only in the total energy losses, but also influences on the distribution of the thermal losses in the volume.

The high power behavior of piezotransducers is very sensitive to loading conditions and differs for 1) constant voltage, 2) constant current, 3) constant vibration velocity and 4) constant input power.

The results [33] clearly concluded that compared to the resonance, the anti-resonance exhibits a higher mechanical quality factor Q_m and the same vibration amplitude/velocity under a smaller input electrical power and lower heat generation. This may suggest a superiority of the anti-resonance application, typically for ultrasonic motor and transformer.

The [33] results may be explained in such a way. When piezoelectric sample is excited by constant voltage the instantaneous power in sample is increased at resonance frequency in many times in respect to off-resonant case. And when sample is excited by constant current the instantaneous power in sample is decreased at resonance frequency in that ratio. Thus, the reason of curve nonlinearity at constant voltage and its absence at constant current is lower level of an instantaneous power.

Modeling of piezoelectric element vibrations by *R, C, L* famous value elements permits to study these influence on resonant/anti-resonant frequencies as well as full conductivities.

Accounting only constant values of dielectric, elastic and piezoelectric loss tangents in calculations do not conflicts with analytic and experimental results.

Acknowledgements

The author thanks S.P. Timoshenko Institute of Mechanics, Nat. Acad. Sci. of the Ukraine for supports these investigations. He would wish like to acknowledge Prof O.I. Bezverkhy (Ukraine) for useful consultations and Dr A.V. Mezheritsky (USA) for important information.

References

1. *Berlincour D.A., Curran D.R. and Jaffe H.* Piezoelectric and piezomagnetic materials and their function in transducers. In Physical acoustics, vol.1. W.P. Mason ed. New York, Academic Press, 1964, pt. A. pp. 169 – 270.
2. *Butterworth S.* On electrically maintained vibrations // Proc. Phys. Soc. (London). – 1915. – Vol. 27. – pp. 410 – 424.
3. *Cady W.G.* Theory of longitudinal vibrations of viscous rods // Phys. Rev. – 1922. – Vol. 19, no 1. – pp. 1 – 6.
4. *Dye D.E.* The piezoelectric quartz resonator and its equivalent circuit // Proc. Phys. Soc. (London). – 1926. – Vol. 38. – pp. 399 – 453.
5. *Dyke Van S.* The electric network equivalent of piezoelectric resonators // Phys. Rev. – 1925. – Vol. 25. – p. 895(A).
6. *Glozman I.A.* Pjezokeramika [Piezoceramics], Moscow, Energhiya, 1972. – 288 p. (Rus)
7. *Holland R.* Representation of dielectric, elastic and piezoelectric losses by complex coefficients // IEEE Trans. SU. – 1967. – Vol. SU-14. pp.18 – 20.
8. IRE Standards on Piezoelectric Crystals: Measurements of Piezoelectric Ceramics. 1961 // Proc. IRE. – 1961. – Vol. 49. – pp. 1161 – 1169.
9. *Jaffe B., Cook W.R. and Jaffe H.* Piezoelectric ceramics. – London, Academic Press: 1971.
10. *Kalashnikov A.M. and Stepuk Ya.V.* Osnovy radiotechniki I radiolokatsiji, koljebatjel"nyje sistjemy [Bases of radio-engineering and radiolocation, vibrating systems]. Moscow, Voyeniz, 1962. 368 p. (Rus)

11. *Karlash V.L.* Vlijanije dissipatsiyi energhiyi na amplitudno-chastotnyje charakteristiki polnoy provodimosti tonkogo pjezokeramidheskogo diska [Influence of energy dissipation on amplitude-frequency characteristics of thin piezoceramic disk full conductivity] // Electrichestvo. – 1984. –no 4. – pp. 59 – 61. (Rus)
12. *Karlash V.L.* Dissipatsiya energhiyi pri koljebaniyakh tonkikh pjezokeramidheskikh kruglykh plastin [Energy dissipation at vibrations of thin piezoceramic circular plates] // Prikladnaya mechanika – 1984. – Vol. 20, no 5. – pp. 77 – 82. (Rus)
13. *Karlash V.L.* Resonant electromechanical vibrations of piezoelectric plates // Int. Appl. Mech. – 2005. – Vol. 41, no 7. – pp. 709 – 747.
14. .*Karlash V.L.* Longitudinal and lateral vibrations of a plate piezoceramic transformer // U. J. Phys. – 2006. – Vol. 51, no 10. – pp. 985 – 991.
15. *Karlash V.L.* Particularities of amplitude-frequency characteristics of admittance of thin piezoceramic half-disk // Int. Appl. Mech. – 2009. – Vol. 45, no10. – pp. 647 – 653.
16. *Karlash V.L. and Ulitko A.F.* Metod issljedovanija medhanicheskilh naprjazheniy v koljebljushchikhsja pjezokeramidheskikh tjelakh [Method of mechanic stress investigation in vibrating piezoceramic bodies] // Eelectrichestvo. – 1976. – no 11. - pp. 82 – 83. (Rus)
17. .*Karlash V.L.* Electroelastic vibrations and transformation ratio of a planar piezoceramic transformer // J. Sound Vib. – 2004. – Vol. 277. –pp. 353 – 367.
18. .*Karlash V.L.* Longitudinal and lateral vibrations of a planar piezoceramic transformer // Jpn. J. Appl. Phys. – 2005. – Vol. 44, no 4A. – pp. 1852 – 1856.
19. *Karlash V.L.* Planar electroelastic vibrations of piezoceramic rectangular plate and half-disk // Int. Appl. Mech. – 2007. – Vol. 43, no 5. – pp. 547 – 553.
20. *Katz H.W.* (ed) Solid State Magnetic and Piezoelectric Devices/ New York, Willey, - 1959.
21. *Land C.E., Smith G.W and Westgate C.R*. The dependence of small-signal parameters of the ferroelectric ceramic resonators upon state of polarization // IEEE Trans. Sonics and Ultrasonics. – 1964. Vol. SU-11. - pp. 8 –19.
22. *Mason W.P.* Location of hysteresis phenomena in Rochelle salt // Phys. Rev. – 1940. – Vol. 58. – pp. 744 – 756.
23. *Martin G.E.* Dielectric, piezoelectric and elastic losses in longitudinally polarized segmented ceramic tubes // U.S. Navy J. Underwater Acoustics. – 1965. – Vol. 15. – pp. 329 – 332.
24. *Mezheritsky V.* Electrical measurements of a high-frequency, high-capacitance piezoceramic resonator with resistive electrodes // IEEE Trans UFFC, 2005, Vol. 52, no 8, pp. 1229 – 1238.
25. *Mezheritsky A.V.* Quality factor of piezoceramics, Ferroelectrics, 2002, Vol. 266, pp. 277 – 304.
26. *Mezheritsky A.V.* Elastic, dielectric and piezoelectric losses in piezoceramics; how it works all together // IEEE Trans UFFC. – 2004. – Vol. 51, no 6. – pp. 695 – 797.
27. *Quimby S.L.* On the experimental determination of the viscosity of vibrating solids // Phys. Rev. –1925. – Vol. 38. - pp. 568 – 582.
28. .*Shul'ga N.A. and Bolkisev A. M.* Koljebaniya pjezoelektridheskikh tjel [The Vibrations of Piezoelectric Bodies] / Kiev, Naukova dumka,. – 1990. (Rus)
29. *Shul'ga M.O. and Karlash V.L.* Rezonansni elektromekhanichni kolyvannja pjezoelektridheskikh plastyn [Resonant electromechanic vibrations of piezoelectric plates] /, Kyiv, Naukova dumka, – 2008. 272 p.(Ukr)
30. *Smith J.G.* Iterative method for accurate determination of real and imaginary parts of materials coefficients of piezoelectric ceramics // IEEE Trans. SU. – 1976. – Vol. SU-23, no 6. – pp. 393 – 402.
31. *Uchino K. and Hirose S.* Loss mechanisms in piezoelectrics: how to measure different losses separately // IEEE Trans UFFC. – 2001. –Vol. 48, no1 pp. 307 – 321
32. *Uchino K., Zheng J.H., Chen Y.H.* et al Loss mechanisms and high power piezoelectrics . – J. Mat. Sci – 2006. - Vol. 41, pp 217 – 228.
33. *Ural S.O., Tunodemi S., Zhuang Yu. and Uchino K.* Development of a high power piezoelectric Characterization system and its application for resonance/antiresonance mode characterization. – Jpn. J. Appl. Phys. – 2009. - Vol. 48 056509
34. US Patent 439 992 1954 / Rosen C. A.- 29.06.1954.
35. *Voigt W.* Lehrbuch der kristallphysik. Leipzig , B.G.Teubner.–1910
36. Zherebtsov I.P. Radiotekhnika [Radioengineering] Moscow, Svyaz' – Sov. Radio. – 1965. – 656 p. (Rus)

Поступила в редакцию 26 декабря 2013 г.

УДК 534.121.1

В.Л. Карлаш, д-р. тех. наук

Інститут механіки ім. С.П. Тимошенко НАН України,

вул. Нестерова, 3, м. Київ, 03057, Україна, e-mail: karlashv@ukr.net.

Втрати енергії в п'єзокерамічних резонаторах і їх вплив на характеристики коливань

Стаття присвячена анадізу сучасних досягнень у проблемі втрат енергії в п'єзокерамічних резонаторах. Паралельно презентується нова проста методика експериментального визначення коефіцієнтів втрат енергії та зв'язку і подається думка автора, чому механічна добротність на резонансі та антирезонансі є різною. Причина полягає у „затиснутій" ємності та у величині коефіцієнта електромеханічного зв'язку. Чим кращий електромеханічний зв'язок, тим дужче „затиснута" ємність і тим вищий її вплив на антирезонансну частоту й добротність. Бібл. 36, рис. 4., табл. 3.

Ключові слова: *п'єзокерамічні резонатори, втрати енергії, електромеханічні коефіцієнти зв'язку, резонансні / анти-резонансні механічні якості.*

УДК 534.121.1

В.Л. Карлаш, д-р. тех. наук

Институт механики им. С.П. Тимошенко НАН Украины,

ул. Нестерова, 3, г. Киев, 03057, Украина, e-mail: karlashv@ukr.net.

Потери энергии в пьезокерамических резонаторах и их влияние на характеристики колебаний

Статья посвящена анализу современных достижений в проблеме потерь энергии в пьезокерамических резонаторах. Параллельно презентуется новая простая методика экспериментального определения коэффициентов потерь энергии и святи и приводится мнение автора, почему механическая добротность на резонансе и антирезонансе разная. Причина состоит в «зажатой» емкости и в величине коэффициента электромеханической связи. Чем лучше электромеханическая связь, тем сильнее «зажата» емкость и тем выше ее влияние на антирезонансную частоту и добротность. Библ. 36, рис. 4., табл. 3.

Ключевые слова: *пьезокерамические резонаторы, потери энергии, электромеханические коэффициенты связи, резонансные/анти-резонансные механические качества.*

Список использованных источников

1. *Berlincour D.A., Curran D.R. and Jaffe H.* (1964), «Piezoelectric and piezomagnetic materials and their function in transducers». In Physical acoustics, Vol.1. W. P. Mason ed. New York, Academic Press, pt. A. pp. 169 – 270.
2. *Butterworth S.* (1915), "On electrically maintained vibrations". Proc. Phys. Soc. (London), Vol. 27, pp. 410 – 424.
3. *Cady W.G. (*1922), "Theory of longitudinal vibrations of viscous rodsy". Phys. Rev., Vol. 19, no 1, pp. 1 – 6.
4. *Dye D.E.* (1926), "The piezoelectric quartz resonator and its equivalent circuit". Proc. Phys. Soc. (London), Vol. 38, pp. 399 – 453.
5. *Dyke Van S.* (1925), "The electric network equivalent of piezoelectric resonators". Phys. Rev., Vol. 25, p. 895(A).
6. *Glozman I.A.* (1972), "Pjezokeramika [Piezoceramics]". Moscow, Energhiya. P.288. (Rus)
7. *Holland R.* (1967), "Representation of dielectric, elastic and piezoelectric losses by complex coefficients". IEEE Trans. SU., Vol. SU-14. pp.18 – 20.

8. “IRE Standards on Piezoelectric Crystals: Measurements of Piezoelectric Ceramics”, (1961). Proc. IRE. Vol. 49, pp. 1161 – 1169.
9. *Jaffe B., Cook W.R. and Jaffe H.* (1971), “Piezoelectric ceramics”. London, Academic Press:.
10. *Kalashnikov A.M. and Stepuk Ya.V.* (1962), “Bases of radio-engineering and radiolocation vibrating systems”, Moscow, Voyeniz, p. 368. (Rus)
11. *Karlash V.L.* (1984), “Influence of energy dissipation on amplitude-frequency characteristics of thin piezoceramic disk full conductivity”, Electrichestvo, no 4, pp. 59 – 61. (Rus)
12. *Karlash V.L.* (1984), “Energy dissipation at vibrations of thin piezoceramic circular plates”, Prikladnaya mechanika, Vol. 20, no 5. pp. 77 – 82. (Rus)
13. *Karlash V.L. (*2005), “Resonant electromechanical vibrations of piezoelectric plates”, Int. Appl. Mech., Vol. 41, no 7, pp. 709 – 747.
14. .*Karlash V.L.* (2006), “Longitudinal and lateral vibrations of a plate piezoceramic transformer”, U.J. Phys., Vol. 51, no 10, pp. 985 – 991.
15. *Karlash V.L.,* (2009), “Particularities of amplitude-frequency characteristics of admittance of thin piezoceramic half-disk”, Int. Appl. Mech., Vol. 45, no10, pp. 647 – 653.
16. *Karlash V.L. and Ulitko A.F.* (1976), “Method of mechanic stress investigation in vibrating piezoceramic bodies”, Eelectrichestvo, no 11, pp. 82 – 83. (Rus)
17. .*Karlash V.L.* (2004), “Electroelastic vibrations and transformation ratio of a planar piezoceramic transformer”, J. Sound Vib., Vol. 277, pp. 353 – 367."
18. .*Karlash V.L.* (2005), “Longitudinal and lateral vibrations of a planar piezoceramic transformer”, Jpn. J. Appl. Phys., Vol. 44, no 4A, pp. 1852 – 1856.
19. *Karlash V.L.* (2007), “Planar electroelastic vibrations of piezoceramic rectangular plate and half-disk”, Int. Appl. Mech., Vol. 43, no 5, pp. 547 – 553.
20. *Katz H.W.* (1959), “Solid State Magnetic and Piezoelectric Devices”, New York, Willey.
21. *Land C.E., Smith G.W and Westgate C.R.* (1964), “The dependence of small-signal parameters of the ferroelectric ceramic resonators upon state of polarization”, IEEE Trans. Sonics and Ultrasonics, 1964. Vol. SU-11. - pp. 8 –19.
22. *Mason W.P.* (1940), “Location of hysteresis phenomena in Rochelle salt”, Phys. Rev., Vol. 58, pp. 744 – 756.
23. *Martin G.E.* (1965), “Dielectric, piezoelectric and elastic losses in longitudinally polarized segmented ceramic tubes”, U.S. Navy J. Underwater Acoustics, Vol. 15, pp. 329 – 332.
24. *Mezheritsky V.* (2005), “Electrical measurements of a high-frequency, high-capacitance piezoceramic resonator with resistive electrodes”, IEEE Trans UFFC, Vol. 52, no 8, pp. 1229 – 1238.
25. *Mezheritsky A.V.* (2002), “Quality factor of piezoceramics”, Ferroelectrics, Vol. 266, pp. 277 – 304.
26. *Mezheritsky A.V.* (2004), “Elastic, dielectric and piezoelectric losses in piezoceramics; how it works all together”, IEEE Trans UFFC, Vol. 51, no 6, pp. 695 – 797.
27. *Quimby S.L.* (1925), “On the experimental determination of the viscosity of vibrating solids”, Phys. Rev., Vol. 38, pp. 568 – 582.
28. .*Shul’ga N. A. and Bolkisev A. M.* (1990), “The Vibrations of Piezoelectric Bodies”, Kiev, Naukova dumka. (Rus)
29. *Shul’ga M.O. and Karlash V.L* (2008), “Resonant electromechanic vibrations of piezoelectric plates”, Kyiv, Naukova dumka, p. 272.(Ukr)
30. *Smith J.G.* (1976), “Iterative method for accurate determination of real and imaginary parts of materials coefficients of piezoelectric ceramics”, IEEE Trans. SU., Vol. SU-23, no 6, pp. 393 – 402.
31. *Uchino K. and Hirose S.* (2001), “Loss mechanisms in piezoelectrics: how to measure different losses separately”, IEEE Trans UFFC, Vol. 48, no1, pp. 307 – 321
32. *Uchino K., Zheng J. H., Chen Y. H.* (2006), “et al Loss mechanisms and high power piezoelectrics”, J. Mat. Sci, Vol. 41, pp 217 – 228.
33. *Ural S.O., Tunodemi S., Zhuang Yu. and Uchino K.,* (2009), “Development of a high power piezoelectric Characterization system and its application for resonance/antiresonance mode characterization“, Jpn. J. Appl. Phys., Vol. 48 056509.
34. *Rosen C.A.* (1954), US Patent 439 992.
35. *Voigt W.* (1910), “Lehrbuch der kristallphysik”, Leipzig, B.G.Teubner.
36. *Zherebtsov I.P.* (1965), “Radio-engineering”, Moscow, Svyaz’, Sov. Radio, 656 p. (Rus)